Liquid Crystalline Ionomers Containing Azobenzene Mesogens: Phase Stability, Photoinduced Birefringence, and Holographic Grating

Qi Bo,[†] Artashes Yavrian,[‡] Tigran Galstian,[‡] and Yue Zhao*,[†]

Département de Chimie, Université de Sherbrooke, Sherbrooke, Québec, Canada J1K 2R1, and Centre d'Optique, Photonique et Lasers, Département de Physique, Université Laval, St-Foy, Québec, Canada G1K 7P4

Received December 20, 2004; Revised Manuscript Received February 14, 2005

ABSTRACT: Liquid crystalline (LC) ionomers containing azobenzene mesogens and three transition metal ions (Cu^{2+}, Zn^{2+}, and Mn^{2+}) were prepared and characterized. Metal ions were found to exert significant effects on the photoinduced orientation of azobenzene mesogens and on the diffraction efficiency of holographic gratings. Using methacrylic acid for neutralization with metal ions, as compared with the copolymer with no metal, ionomers of Zn and Mn showed increased photoinduced birefringence and higher diffraction efficiency of birefringence gratings obtained by excitation with spatially modulated light polarization. By contrast, ionomers with Cu showed the opposite effects. As a whole, the behavior of photoinduced birefringence and holographic grating appears to be correlated with the thermal stability of the LC phase formed by azobenzene mesogens in the ionomer. Some new thoughts are discussed regarding the effect of metal and their ionic aggregates on the clearing temperature of LC ionomers. The interest for further exploring azobenzene LC ionomers is demonstrated by the finding that the insertion of a small amount of certain metal ions could be an effective means to improve or to tune the properties of azobenzene polymers.

Introduction

Liquid crystalline (LC) ionomers are of interest because they have properties characteristic of both LC and ion-containing polymers, namely, the formation of LC phases and the existence of ionic aggregates.[1−9] The incorporation of a small amount of metal ions in LC polymers (LCPs) is a means to alter the properties. For instance, Barmatov and co-workers showed that the presence of copper ions could make the LC ionomers antiferromagnetic[6] and that the insertion of cobalt ions in a chiral nematic LCP could prevent the untwisting of the helical pitch with decreasing the temperature.[9] Zentel et al. utilized LC ionomers in conjunction with amorphous polyelectrolytes to prepare multilayers.[5] And our group used LC ionomers as a model system to investigate the effect of chain mobility on the magnetic field-induced orientation of mesogens and its coupling with the flexible spacer and chain backbone.[3] Obviously, the most direct consequence of having ionic aggregates in LCPs is the possible influence on the order and stability of the LC phases formed by mesogens. It is now known that the presence of metal ions can either increase or decrease the LC-to-isotropic phase transition temperature,[1,2,6−9] i.e., the clearing temperature, which depends on a number of parameters such as the nature of metal ions, the chemical structure of LCP, and the position of the metal-neutralized acid groups with respect to polymer chain backbone.[9]

If metal ions are introduced in a LCP with azobenzene mesogens in side groups, the ionic aggregates may exert effects not only on the LC phases but also on the photoinduced orientation of azobenzene mesogens under linearly polarized irradiation, which is at the origin of the great interest given to the development of a variety of azobenzene-containing polymers.[11−15] In the present work, we have studied azobenzene LC ionomers. Of the different methods reported for the preparation of LC ionomers, perhaps the easiest one consists of incorporating some acrylic or methacrylic acid units in a side-chain liquid crystalline polymer (SCLCP) through radical copolymerization and then neutralizing the acid groups with metal ions (partially or completely).[1] In the first part of this paper, we report the synthesis of two series of azobenzene LC ionomers using this method. On the basis of the characterization results, discussions are given to present some new thoughts on how ionic aggregates may decrease or increase the clearing temperature depending on the position of ions with respect to polymer chain backbone. The second part of the paper discusses the photoinduced birefringence and the recording of holographic gratings in azobenzene LC ionomers. The results point to a correlation between the increased thermal stability of LC phases and the enhanced photoinduced orientation of azobenzene mesogens in the presence of some metal ions.

Experimental Section

Figure 1 shows the chemical structures of the two series of azobenzene LC ionomers prepared. Methacrylate-based random copolymers were first obtained through radical copolymerization of the azobenzene monomer 6-[4-(4-methoxyphenylazo)phenoxy]hexyl methacrylate (Azo) with either methacrylic acid (MA) or 4-(6-(methacryloyloxy)hexyloxy)benzoic acid (BA). They are referred to as Azo-*y*MA and Azo-*y*BA, respectively, where *y* is the mole fraction of the acid comonomer units. After partial neutralization of the carboxylic acid groups with metal cations through reaction between copolymer and metal acetate, azobenzene LC ionomers of Azo-($y-z$)MA-0.5*z*Metal and Azo-($y-z$)BA-0.5*z*Metal were obtained, where *z* is the mole fraction of metal neutralized carboxylate groups and 0.5*z* is the mole fraction of one of the three used metal ions: Cu^{2+}, Zn^{2+}, and Mn^{2+}. Of these three transition metals, Cu^{2+} and Zn^{2+} were chosen because their ionomers were much studied in the

[†] Université de Sherbrooke.
[‡] Université Laval.
* Corresponding author: e-mail yue.zhao@usherbrooke.ca.

10.1021/ma0473869 CCC: $30.25
Published on Web 03/18/2005

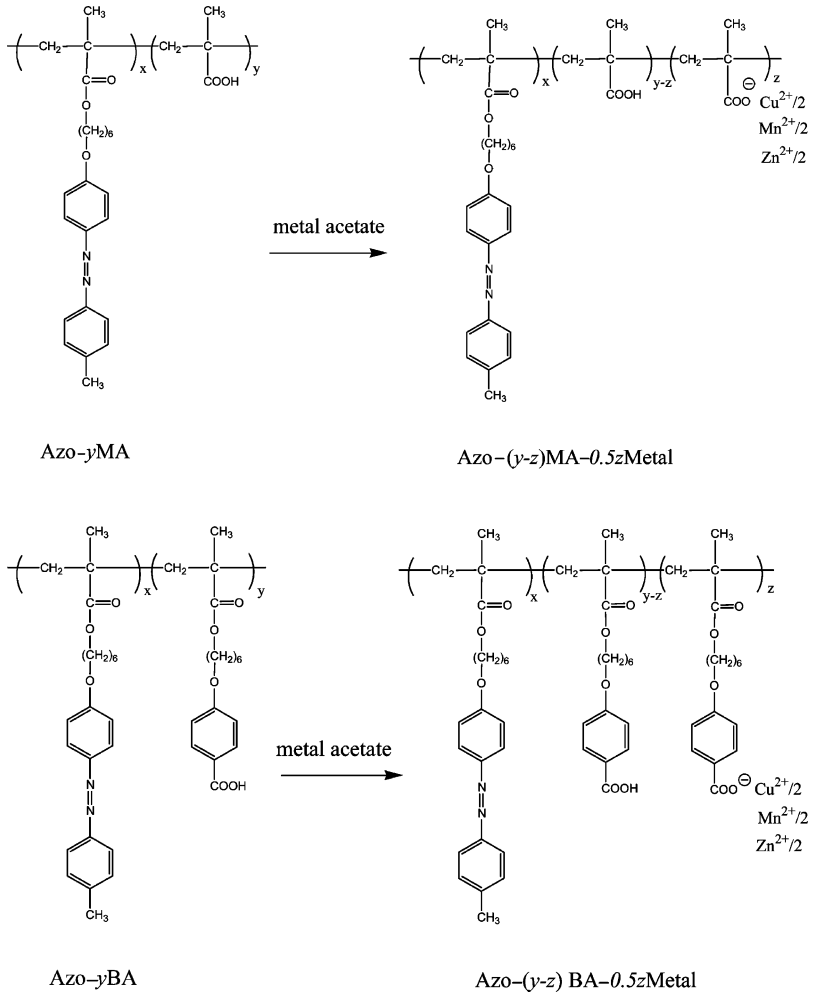

Figure 1. Chemical structures of two series of copolymers and their corresponding ionomers (see text for the explanation of the acronym).

literature,[6,8,10] while Mn^{2+} was also picked from other transition metals since the available manganese acetate made easy the preparation of its ionomer. More experimental details are given below.

Materials. *p*-Anisidine (99%), phenol (99%+), 6-chloro-1-hexanol (96%), methacryloyl chrloride (97%), copper(II) acetate (98%), zinc acetate dihydrate (98%+), manganese(II) acetate (98%), and calcium hydride (90−95%) were used as received from Aldrich. Sodium nitrate (ACS norms) and sodium hydroxide were purchased from Fisher Chemicals and used without further purification. Potassium iodide (Baker Chemicals), potassium carbonate anhydrous (EMD), and sodium sulfate anhydrous (ACS, Anachemia) were also used as received. AIBN (Polysciences) was recrystallized from ethanol and dried under reduced pressure at room temperature before use as initiator for radical polymerizations. Triethylamine was refluxed with calcium hydride and distilled before use. All solvents were commercially available and purified using standard procedures. For the monomers, methacrylic acid (Aldrich, 99%) was distilled before use, while Azo and BA were synthesized using methods reported in the literature.[16]

Synthesis of Random Copolymers. Different feed ratios of the azobenzene monomer with either MA or BA were used. In all cases, weighed amounts of the two monomers, together with AIBN, were dissolved in anhydrous THF, with a total monomer concentration of 30 wt %. The concentration of AIBN was 2 wt % with respect to the amount of monomers. After three freeze−thaw−vacuum cycles, the solution was heated to 60−70 °C for 24 h of polymerization. Afterward, the reaction mixture was precipitated in cold methanol three times, and the collected polymer was dried under reduced pressure (yield: 50−60%).

Preparation of Ionomers. The ionomers were prepared using the following procedure.[6] A solution of metal acetate in ethanol (0.5 wt %) was added to a THF solution of the copolymer (1 wt %) with stir. The reaction continued for 4 h at room temperature. The solution was then filtered through a 0.45 μm Teflon membrane to remove any particles. After most solvent was evaporated under reduced pressure the sample was further dried in a vacuum at 100 °C for 1 h.

Characterizations. ^{1}H NMR spectra were recorded on a Bruker spectrometer (300 MHz, AC300). Molecular weights and polydispersities were measured by gel permeation chromatography (GPC) using a Waters system equipped with a refractive index and a photodiode array detector; THF was used as the eluent (elution rate, 0.5 mL/min), and polystyrene standards were used for calibration. Textures were examined on a Leitz DMR-P polarizing microscope equipped with an Instec hot stage. Phase transition temperatures were measured using a Perkin-Elmer DSC-7 differential scanning calorimeter with heating and cooling rate of 10 °C min^{-1}. UV−vis and infrared spectra were recorded with a HP 8452A spectrophotometer and a Bomen MB-102 FTIR spectrometer (CaF_2 crystal used for casting the films). X-ray diffraction measurements were conducted on a Bruker diffractometer with a two-dimensional position-sensitive wire-grid detector (Bruker AXS).

Optical Measurements. Two types of optical measurements were carried out in this work. First, for the measurement of photoinduced birefringence performed at room temperature, a typical polarimetric optical setup similar to that described elaswhere[17] was utilized. Namely, a thin film was placed between two crossed polarizers; a plane-polarized Ar^+ ion laser (λ = 488 nm) was applied as the excitation beam,

Table 1. Characteristics of Polymers[a]

polymer	$\overline{M}_n$	$\overline{M}_w/\overline{M}_n$	phase transitions (°C)	ΔH_{sn} (J/g)	ΔH_{ni} (J/g)
PAzo	9.0×10^3	1.8	G61S89N129I	1.91	1.50
Azo-0.26MA	1.1×10^4	2.1	G65N119I		2.52
Azo-0.40MA	1.7×10^4	2.3	G72N116I		1.09
Azo-0.52MA	4.0×10^4	1.5	G76		
Azo-0.26BA	0.8×10^4	1.9	G58N112I		1.97
Azo-0.50BA	4.0×10^4	2.5	G74N131I		2.91
Azo-0.87BA	0.5×10^4	1.1	G80N136I		4.74

[a] G = glass transition, S = smectic phase, N = nematic phase, and I = isotropic phase.

with a small incident angle to the film. The excitation intensity was adjusted to be about 100 mW/cm^2, and the polarization was set at 45° with respect to the crossed polarizers. The anisotropy photoinduced in the area exposed to the Ar^+ laser beam led to the polarization variation of a probe light with normal incidence (HeNe laser, 633 nm, 4 mW) that had little effects on the isomerization of azobenzene mesogens. Because of the crossed polarizer and analyzer, this polarization change was transferred into the intensity variation measured by means of a photodiode detector placed behind the analyzer, which allowed the photoinduced birefringence to be calculated. In the setup, a second photodiode was also used to detect changes in intensity of the probe light before passing through the second polarizer in order to make sure that the measured transmission changes were not caused by scattering or absorption of the sample. Second, the same optical setup was modified to have a typical configuration for the recording of holographic gratings.[18] Namely, a beam splitter was used to produce two coherent beams from the Ar^+ laser. The interference pattern was produced by two beams that were orthogonally circularly polarized by means of a quarter-wave plate. The resulting interference field had spatial modulation of polarization; that is, the intensity of light was almost uniform while the direction of the resulted linear polarization of light was periodically rotating with respect to the vector of the grating. The crossing angle of two recording beams was adjusted to yield gratings with various periods; a period of 5 μm was used unless otherwise stated. The power per recording beam (with a diameter of about 4 mm) was chosen to be either 50 or 150 mW/cm^2, which was measured using a powermeter placed in front of the film. The HeNe laser beam, polarized parallel to grating fringes, was used as probe to monitor the grating formation dynamics through the simultaneous measurement of intensities of the transmitted (I_t) and the first-order diffracted (I_d) beams. The first-order diffraction efficiency η was calculated as the ratio of I_d over I_t^o, where I_t^o is the transmitted intensity before the recording of grating.

Results and Discussion

I. Thermal Stability of Liquid Crystalline Phases. The characteristics of the two series of random copolymers are summarized in Table 1. The actual compositions, which differed slightly from the feed ratios, were determined using ^{1}H NMR and UV−vis spectroscopy. In the latter case, dilute solutions of the azobenzene polymer, PAzo, were used to obtain a calibration curve of azobenzene absorption at 360 nm as a function of the concentration, which was then used to determine the content of Azo units in random copolymers by assuming the same extinction coefficient of azobenzene. For each sample, both techniques yielded similar results, and the average value was reported in Table 1. In contrast to PAzo which has a nematic and a smectic-A phase, copolymers of Azo-0.26MA and Azo-0.40MA show only a nematic phase, and their clearing temperature T_{ni} decreases as the mole fraction of MA increases. It is no surprise that the presence of nonmesogenic MA units

Table 2. Characteristics of Ionomers

ionomer	phase transitions (°C)	ΔH_{ni} (J g^{-1})	ΔS_{ni} (J K^{-1} g^{-1})
Azo-0.23MA-0.015Cu	G53N121I	1.54	3.91×10^{-3}
Azo-0.23MA-0.015Zn	G51N133I	1.17	2.88×10^{-3}
Azo-0.23MA-0.015Mn	G52N142I	1.05	2.53×10^{-3}
Azo-0.20MA-0.03Cu	G60N105I	1.69	4.47×10^{-3}
Azo-0.20MA-0.03Zn	G59N126I	1.65	4.13×10^{-3}
Azo-0.20MA-0.03Mn	G79N139I	1.27	3.08×10^{-3}
Azo-0.14MA-0.06Cu	G68N106I	2.74	9.98×10^{-3}
Azo-0.14MA-0.06Zn	G52N138I	0.76	1.85×10^{-3}
Azo-0.14MA-0.06Mn	G62N152I	0.37	8.71×10^{-4}
Azo-0.20BA-0.03Cu	G66N112I	2.32	6.03×10^{-3}
Azo-0.20BA-0.03Zn	G61N106I	1.52	4.01×10^{-3}
Azo-0.20BA-0.03Mn	G61N112I	1.29	3.35×10^{-3}
Azo-0.14BA-0.06Cu	G49N103I	1.51	4.02×10^{-3}
Azo-0.14BA-0.06Zn	G51N103I	0.92	2.45×10^{-3}
Azo-0.14BA-0.06Mn	G50N102I	1.92	5.12×10^{-3}

reduces T_{ni} and eventually suppresses the nematic phase when the MA content reaches about 52% (Azo-0.52MA). For the series of Azo-BA, all copolymers show a nematic phase as confirmed by X-ray scattering measurements, but the depression of T_{ni} is observed only for Azo-0.26BA. T_{ni} actually increases at higher concentrations of BA. This different behavior is explained by the formation of hydrogen-bonded dimers of BA moieties that are mesogenic. The homopolymer BA has the highest clearing temperature of about 170 °C.

Random LC copolymers of Azo-0.26MA and Azo-0.26BA, which have the same content of acid units within experimental errors, were chosen to prepare ionomers through partial neutralization using three transition metals: Cu, Zn, and Mn. Table 2 lists the measured nematic-to-isotropic phase transition temperatures (T_{ni}) and enthalpies (ΔH_{ni}) of the azobenzene LC ionomers prepared; their phase transition entropies (ΔS_{ni}) calculated from $\Delta H_{ni}/T_{ni}$ are also shown. The mole fraction of metal-neutralized acid groups in the acronym for each sample is based on the amount of metal acetate used assuming a complete reaction, which is reasonable under the used conditions.[8] Infrared spectra confirmed the proportional increase of the amount of metal ions among the different series, as shown by the example in Figure 2 for Azo-MA-Zn. The absorption band of carboxylic acid dimers at 1700 cm^{-1} decreases as the content of Zn^{2+} increases, which indicates the disruption of H-bonded dimers by ionic aggregates. To better illustrate the trends of the influence of metal ions on the thermal stability of LC phases, Figure 3 plots the clearing temperature as a function of mol % of metal for the two series of azobenzene LC ionomers. The two

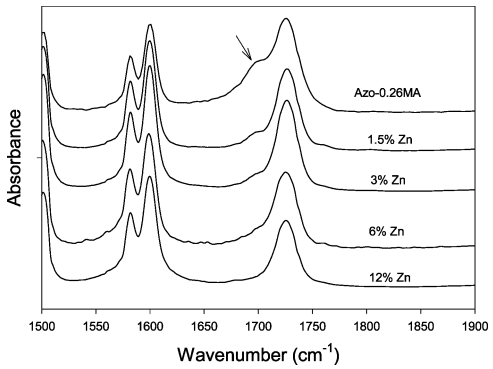

Figure 2. Infrared spectra in the 1500−1900 cm^{-1} region for Azo-0.26MA and its ionomers with different contents (mol %) of Zn^{2+}.

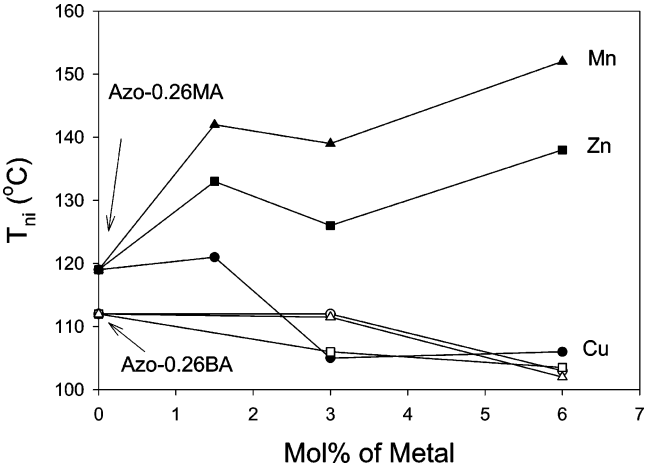

Figure 3. Clearing temperature T_{ni} vs metal content for two series of ionomers prepared from Azo-0.26MA (closed symbols) and Azo-0.26BA (open symbols): Mn (triangle), Zn (square), and Cu (circle).

copolymers with no metal have a similar concentration of acid comonomeric units and a comparable clearing temperature. However, the insertion of metal ions resulted in very different effects on the thermal stability of LC phases formed by the same azobenzene mesogens. For the Azo-MA-Metal series, T_{ni} is increased by the presence of Zn^{2+} and Mn^{2+} ions, while it decreases with Cu^{2+}. Quite surprisingly, the rise in T_{ni} can be as important as 30 °C with 6% of Mn^{2+}. By contrast, for the Azo-BA-Metal series, the clearing temperature of ionomers displays a slight decrease for the three metals. For both systems, apparently neither the increase nor the decrease in T_{ni} is proportional to the amount of metal, but the largest effect is observed at 6 mol % of metal ions.

As mentioned earlier, the influence of metal ions on the clearing temperature of LC ionomers is a complicated issue. Both increase and decrease in T_{ni} were observed for a number of LC ionomers with various metals.[1,2,6−9] In the case of transition metals, in their systematic investigation on LC ionomers (with no azobenzene) using acrylic acid comonomer, Barmatov et al. reported increase in T_{ni} by about 10 °C or less using Co, Ni, and Cu.[6,8] They also used 4-(5-acryloyloxypentyl-1-oxy)benzoic acid, which is similar to BA in this study, as comonomer for metal neutralization[9] and observed a decrease in T_{ni} with Co ions. For our azobenzene LC ionomers, the results in Figure 3 basically show the same trends except for Azo-MA-Cu. Barmatov et al. have attributed the different behaviors to an effect arising from the position of the charged carboxyl groups with respect to polymer chain backbone. According to their interpretations, when charged carboxyl groups are located in the immediate vicinity of chain backbone, which is the case when using acrylic or methacrylic acid comonomers, ionic aggregates could have a structuring effect leading to increase in the clearing temperature (and also to the induction of smectic phase for a nematic LCP).[8] On the other hand, when charged carboxyl groups are distant from chain backbone, which is the case when using comonomers of *n*-alkyloxybenzoic acid, ionic aggregates serve as defects in LC phases, resulting in a decrease in T_{ni}.[9] We feel that it would be of interest to take a look at the effect of position of metal ions from a different angle. In what follows, we propose a thermodynamic analysis to explain

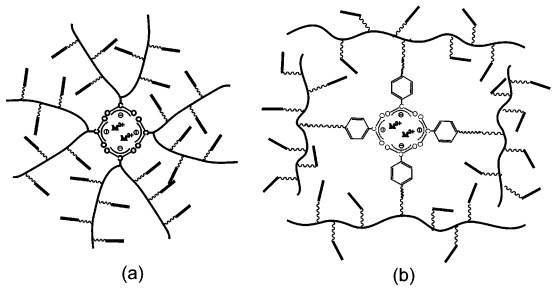

Figure 4. Schematic illustration of polymer chain backbone linked to ionic aggregate (a) in immediate vicinity and (b) through a flexible spacer.

the observed increase and decrease in T_{ni} depending on the chemical structure of the used acid comonomer.

The nematic-to-isotropic phase transition temperature T_{ni} (same for smectic-to-isotropic phase transition T_{si}) is determined by $T_{ni} = \Delta H_{ni}/\Delta S_{ni}$, where ΔH_{ni} and ΔS_{ni} are the differences in enthalpy and entropy between the isotropic and the nematic phase, respectively. The example with Azo-0.14MA-0.06Mn and Azo-0.14BA-0.06Mn provides a striking comparison. Azo-0.14MA-0.06Mn has an ΔH_{ni} about 5 times smaller than that of Azo-0.14BA-0.06Mn, yet the former has a higher T_{ni} than the latter by 50 °C (Table 2). Such a situation is frequently encountered regarding the melting temperature of crystalline polymers.[19] The reason is that the change in entropy ΔS_{ni} is often the decisive factor. As shown in Table 2, Azo-0.14MA-0.06Mn has $\Delta S_{ni} \approx 8.71 \times 10^{-4}$ J $K^{-1}g^{-1}$, which is much smaller than $\Delta S_{ni} \approx 5.12 \times 10^{-3}$ J $K^{-1}g^{-1}$ for Azo-0.14BA-0.06Mn. We suggest that differences in ΔS_{ni} may be a major factor that accounts for the generally observed increase or decrease in T_{ni} for LC ionomers with ionic groups attached directly, like Azo-0.14MA-0.06Mn, or via a flexible spacer, like Azo-0.14BA-0.06Mn, to polymer backbone. Figure 4 schematically illustrates the difference. In the isotropic state of the side-chain mesogens (azobenzene mesogens in the present case), the ionic aggregate, i.e., the multiplet formed by several ion pairs as defined by Eisenberg et al.,[20] that is directly anchored to polymer backbone reduces the mobility of polymer chain more importantly than the ionic aggregate that is connected to polymer backbone through a flexible spacer (alkyl chain).[20] The reduced polymer chain mobility should reduce the degree of freedom of motion for the mesogens and, consequently, result in a loss of their entropy in the isotropic state. A greater reduction in chain backbone mobility will lead to a greater loss of entropy for side-chain mesogens in their isotropic phase, which means a smaller ΔS_{ni} and, consequently, higher T_{ni}. Basically, the point is that in LC ionomers the entropy change associated with the LC-to-isotropic phase transition can be diminished due to the reduced mobility of chain backbone, which is characteristic of random ionomers and is affected by the position of ionic groups as well as the way they are linked to polymer backbone. A smaller ΔS_{ni} for LC ionomers with ionic groups directly attached to chain backbone could thus account for the generally observed increase in T_{ni} from polymer with no metal ions.

From the above analysis, it is obvious that all parameters that affect ΔH_{ni} and/or ΔS_{ni} one way or another affect the clearing temperature, and T_{ni} is determined by the exact balance between the changes in enthalpy and entropy. To this regard, some discus-

sions are worth being made. First, the presence of defects related to ionic aggregates was often given as a general explanation for the decrease in T_{ni}.[1,9] Actually, defects may not necessarily result in a diminished thermal stability of the LC phase. Defects can weaken the cohesion force between mesogens and thus lower ΔH_{ni}, but in the same time, they can also reduce the degree of order of mesogens in the nematic phase; higher entropy in the nematic phase can also result in a smaller ΔS_{ni} and lead to increase in T_{ni}. Second, in the case of LC ionomers containing transition metals, possible coordination interactions between metal ions and mesogens were also suggested to be a factor that influences T_{ni}.[8] Similarly, it can be argued that such specific interactions may affect both ΔH_{ni} and ΔS_{ni}. For instance, if stronger coordination is allowed between metal and mesogens in the isotropic phase, it can decrease ΔH_{ni}, which tends to decrease T_{ni}. But in the same time, stronger coordination in the isotropic phase may also reduce the entropy of mesogens and thus give rise to smaller ΔS_{ni}, which would have the opposite effect on T_{ni}. It is safe to say that the combination of different effects determines the exact balance between ΔH_{ni} and ΔS_{ni}, which varies from system to system depending on many interconnected parameters such as the nature of metal and host polymer, the size, number, and firmness of ionic aggregates, and the length of flexible spacers linking both ionic and mesogenic groups to polymer backbone. What is undoubted is that the presence of ionic aggregates can improve the thermal stability of LC phases for many LC ionomers. When this happens to azobenzene LC ionomers, it may have consequences on the photoinduced anisotropy of azobenzene mesogens as is shown in the second part of the paper.

For the series of Azo-MA-Metal, the origin of the drastically different behavior of Cu ionomers as compared to Mn and Zn ionomers is unclear. An increase in T_{ni} by about 10 °C with 5 mol % of Cu^{2+} was reported for a LC ionomer with biphenyl-based mesogens.[8] We speculate that the observed decrease in T_{ni} for Azo-MA-Cu (Figure 3) may be related to some coordination interactions of the metal ions with azobenzene mesogens. Of the three transition metals used, Cu has the strongest coordination capability. However, UV−vis spectra under irradiation with UV and visible light apparently showed no significant differences for ionomers with the three metals (spectra not shown). In all cases, reversible trans−cis isomerization of azobenzene mesogens in thin films was observed. We also carried out X-ray scattering measurements. Figure 5 shows the scattering patterns at 30 °C of the three ionomers with 6 mol % of metal ions, which were corrected by subtracting the scattering pattern of the polymer with no metal (Azo-0.26MA). The Cu ionomer displays a different scattering profile in that the relative scattering intensity around $2\theta = 20°$, which is associated with liquidlike organization of mesogens and chain segments, is much smaller than those of the Mn and Zn ionomers. Considering the fact that the scattering pattern of Azo-0.26MA, though much less intense than ionomers, shows clearly the broad peak near $2\theta = 20°$, the result seems to indicate that the presence of Mn^{2+} and Zn^{2+}enhances the scattering arising from both large and small spacing while Cu^{2+} in the polymer enhances predominantly the typical small-angle scattering associated with the organization of ionic aggregates.[20] This difference may be indicative of different morphologies

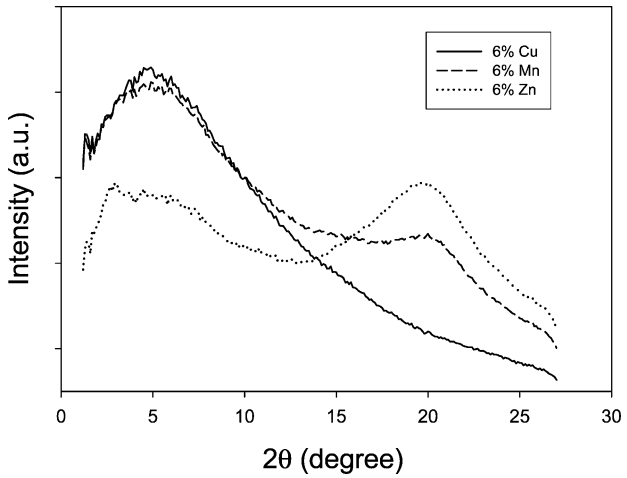

Figure 5. X-ray scattering patterns at room temperature for three ionomers prepared from Azo-0.26MA.

in the three ionomers, though at this point, any further analysis is too speculative to be meaningful.

II. Photoinduced Birefringence and Holographic Grating. The main purpose of exploring azobenzene LC ionomers is to investigate possible effects of metal ions or their aggregates on the properties that are characteristic of azobenzene-containing polymers, one of them being the birefringence induced by linearly polarized light irradiation as a result of the photoinduced orientation of azobenzene moieties. To effectively obtain photoinduced orientation in azobenzene LCPs like the one used in this study, for which azobenzene mesogens in the trans form absorb in the UV region, the film can be treated first with unpolarized UV light to reach the photostationary cis-rich state with azobenzene mesogens in the isotropic phase; then linearly polarized laser excitation at 488 nm, which is close to the absorption of azobenzene moieties in the cis form, can be applied to allow the cis−trans back-isomerization. This process can lead to a quick orientation of azobenzene mesogens while returning back to the trans conformation, in the direction perpendicular to the polarization of the excitation laser.[21] The previous work also suggested that under continuous excitation this quick orientation induction through absorption of cis azobenzene was followed by a slower orientation process due to the absorption of trans azobenzene at 488 nm through repeated trans−cis−trans cycles.[21] In the present study, we utilized this orientation method. The anisotropy due to azobenzene orientation in the exposed area of the film was monitored using a probe light at 633 nm, and changes in transmission of the probe light through the analyzer were used to determine the photoinduced birefringence.

The results for Azo-0.26MA and its ionomers with Cu and Zn are shown in Figure 6. At the three metal contents, ionomers with Zn exhibit higher photoinduced birefringence than the polymer with no metal, while ionomers with Cu show lower photoinduced birefringence. The greatest increase in birefringence was observed with 3 mol % of Zn, whereas the largest decrease was found with 3 mol % of Cu. In all cases, the birefringence reaches a plateau value quite rapidly using the excitation intensity of 100 mW/cm^2. After turning off the excitation laser, the birefringence decreases only slightly due to thermal relaxation, which is characteristic of orientation of azobenzene mesogens induced in LCPs.[13] When circularly polarized excitation

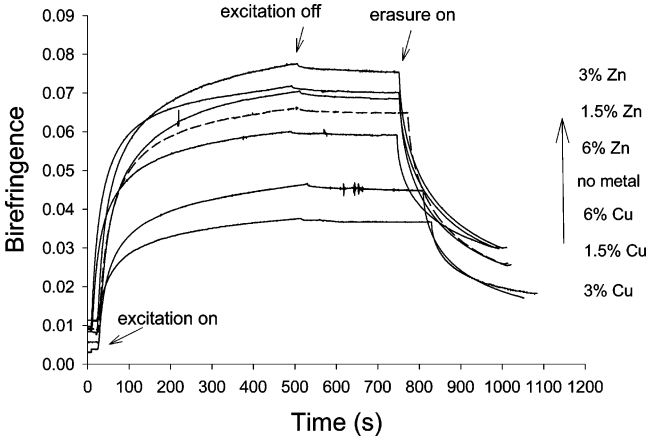

Figure 6. Photoinduced birefringence through Ar^+ laser excitation (488 nm, 100 mW/cm^2) for Azo-0.26MA and its ionomers with different contents (mol %) of Zn^{2+} and Cu^{2+} ions.

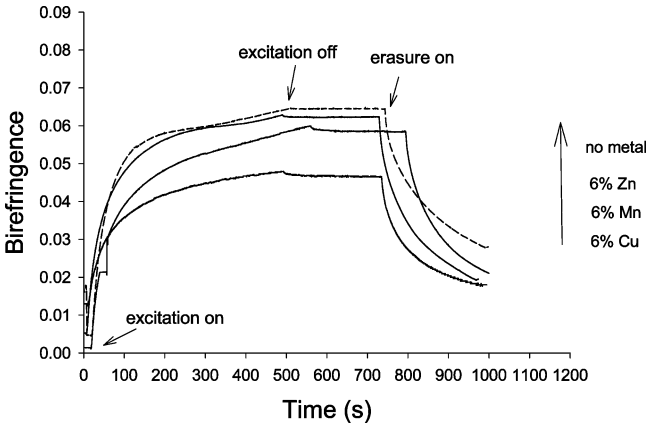

Figure 7. Photoinduced birefringence through Ar^+ laser excitation (488 nm, 100 mW/cm^2) for Azo-0.26BA and its ionomers with 6 mol % of Mn^{2+}, Zn^{2+}, and Cu^{2+} ions.

beam at 488 nm was applied for optical erasure of the birefringence by randomizing the orientation of azobenzene mesogens in the plane perpendicular to the wavevector of the erasing beam, most of the in-plane birefringence could be erased in minutes. Similar to ionomers with Zn, ionomers with Mn also develop greater birefringence than the polymer with no metal (results not shown in Figure 6 for the sake of clarity). For azobenzene LC ionomers prepared from Azo-0.26BA (Table 2), the behavior of photoinduced birefringence is different. Figure 7 compares the birefringence of Azo-0.26BA with the three ionomers containing 6 mol % of Cu, Zn, and Mn. Only the Zn ionomer seems to have a similar birefringence to the polymer, whereas the two others have a smaller birefringence. As discussed earlier, the presence of any of the three metals in Azo-0.26BA has as effect a slight decrease in the clearing temperature (Figure 3).

The above results point to a correlation between the photoinduced birefringence and the thermal stability of the LC phase. Of the two series of ionomers shown in Table 2, those prepared from Azo-MA using Zn and Mn have enhanced thermal stability of the LC phase, and they exhibit increased photoinduced birefringence. By contrast, for other ionomers for which the presence of metal destabilizes or has little effect on the LC phase, they develop either significantly smaller or essentially similar birefringence to the polymer with no metal. The enhancement of the photoinduced birefringence by

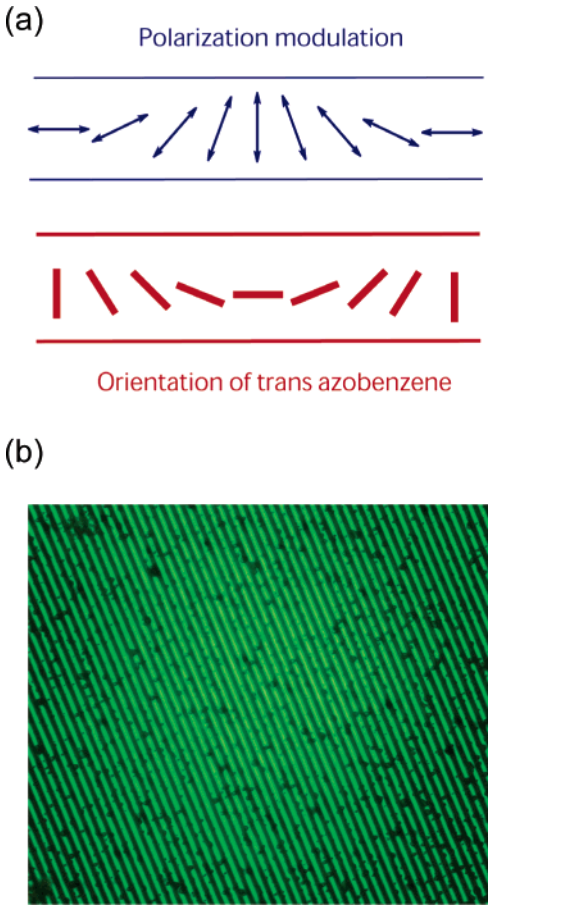

Figure 8. (a) Schematic illustration of an interference pattern with polarization modulation produced by two coherent Ar^{2+} laser beams orthogonally circularly polarized and the corresponding photoinduced orientation of azobenzene mesogens in the trans form. (b) Polarizing optical micrograph of a grating (5 μm period) recorded on a thin film of Azo-0.14MA-0.06Zn (photo size: 214 $\times$ 186 μm).

metal ions is interesting since large photoinduced anisotropy is generally desired for applications.[13,14]

Another attractive property of azobenzene polymers is the ability to form diffraction gratings under excitation of an interference pattern generated by two coherent laser beams. Such a holographic grating can be a scalar grating (between trans and cis isomers), a birefringence grating due to periodic changes in photoinduced orientation of azobenzene moieties, or a surface-relief grating formed as a result of masse transport on the surface of the film.[12,13] We thus performed holographic recording experiments to investigate the possible effects of metal ions on the diffraction efficiency. To obtain birefringence grating whose refractive index modulation is determined by the photoinduced orientation of azobenzene mesogens, the polarization states of the two writing beams (obtained from the Ar^+ laser at 488 nm) were chosen to be orthogonally circularly polarized, which gave rise to an interference pattern with uniform spatial distribution of light intensity, but with rotation of the linear polarization direction along the grating vector, as schematically illustrated in Figure 8a. Since the film used for grating recording was preirradiated with unpolarized UV light to reach maximum cis isomer concentration, as discussed earlier, the interference pattern with such a modulation of plane polarization should initiate cis−trans back-isomerization and orient *trans*-azobenzene moieties in different

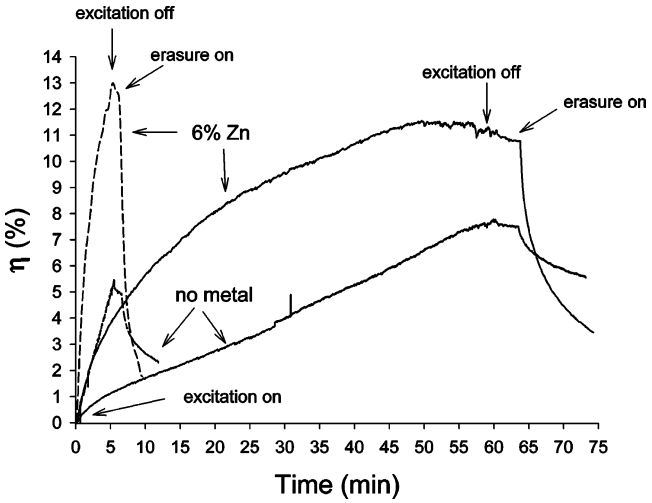

Figure 9. First-order (+1) diffraction efficiency vs time for gratings (5 μm period) recorded in films of Azo-0.26MA and Azo-0.14MA-0.06Zn using two excitation intensities (Ar^+ laser, 488 nm): 1 h excitation with 50 mW/cm^2 per recording beam (solid curves) and 5 min excitation with 150 mW/cm^2 per recording beam (dashed curves). See text for details.

directions dictated by the periodic change in polarization direction of the excitation light, which is also schematized in Figure 8a. Consequently, a birefringence grating should be formed. Under these conditions, birefringence gratings were indeed obtained. Figure 8b shows a 5 μm period grating inscribed on Azo-0.14MA-0.06Zn, viewed on a polarizing optical microscope. The periodic change in orientation direction of azobenzene mesogens was revealed by rotating the grating under crossed polarizers, which resulted in changes between dark and bright fringes. If the presence of metal ions leads to a larger photoinduced birefringence, a greater refractive index modulation for the grating should be expected, giving rise to higher diffraction efficiency. This was indeed observed.

Figure 9 shows the dynamic grating formation process for Azo-0.26MA and its ionomer with 6 mol % of Zn (grating period: 5 μm). Two sets of experimental conditions were used. In one (solid curves), the excitation intensity was 50 mW/cm^2 per recording beam, and the excitation was applied for a long period of 1 h before turning off the excitation for about 5 min, which was followed by an optical erasure of the grating using exposure of the film by one circularly polarized Ar^+ laser beam (the other beam was blocked). In the second (dashed curves), a higher excitation intensity of 150 mW/cm^2 per recording beam was used for 5 min before turning off the excitation for 1 min and the subsequent erasure of the grating. In both cases, the first-order diffraction efficiency of the grating formed in the ionomer is much stronger than that of the grating recorded on the polymer containing no metal. As expected, the grating is mainly formed due to a periodic variation of the direction of photoinduced orientation of azobenzene mesogens. This can be noticed from the optical erasure of the grating under circularly polarized one-beam irradiation as a result of the optical erasure of photoinduced in-plane birefringence (Figure 6). Even with the prolonged excitation of 1 h, the grating remained after the optical erasure appears to be essentially birefringent since the diffracted light was still circularly polarized. To make sure that the observed higher diffraction efficiency (η) was not caused by variations in film thickness (d), the refractive index modulation of the grating, Δn, was estimated from $\eta \approx (\pi d \Delta n/\lambda)^2$, where λ is the wavelength of the probe light (633 nm). This approximation is valid for diffractive gratings in the Raman−Nath regime.[22] Using data in Figure 9 and film thickness carefully measured by means of a profilometer and a digital micrometer, the refractive index modulation Δn is 0.048 for the Zn ionomer and 0.013 for the polymer after 1 h excitation with the lower intensity, and it reaches 0.037 for the ionomer and 0.017 for the polymer after 5 min excitation with the higher intensity. Unambiguously, the presence of 6 mol % of Zn^{2+} ions increases significantly the diffraction efficiency of holographic grating as result of an increased photoinduced birefringence in the ionomer. Another noticeable difference between the Zn ionomer and the polymer is the rate of the optical erasure of grating under one-beam circularly polarized irradiation. The birefringent grating of the ionomer could be erased more quickly than that of the polymer. It is known that photoinduced birefringence produced by azobenzene liquid crystalline polymers is difficult to erase due to the tendency for mesogens to stay aligned and a lower angular mobility, unlike azobenzene amorphous polymers whose photoinduced birefringence can rather easily be erased by circularly polarized light.[13] The results in Figure 9 thus suggest that the LC order, formed by azobenzene mesogens, was reduced in the Zn ionomer as compared to the polymer containing no metal. This indeed is hinted by the much smaller nematic-to-isotropic transition enthalpy of Azo-0.14MA-0.06Zn (0.76 J/g, Table 2) than Azo-0.26MA (2.52 J/g, Table 1).

We then measured the first-order diffraction efficiency for six ionomers prepared from Azo-0.26MA with 3 and 6 mol % of each of the three metals, under similar conditions: about 5 min excitation with the interference pattern (50 mW/cm^2 per pumping beam), followed by turning off the excitation for about 1 min and the subsequent optical erasure of the grating. The film thickness varied around 2 μm. The results are presented in Figure 10. Data for the first 5 min excitation under the same intensity for the polymer with no metal in Figure 9 were also shown for comparison. Even taking into account the variation in film thickness, holographic gratings recorded on ionomers with Zn^{2+} and Mn^{2+} ions display higher diffraction efficiency than the grating of the polymer with no metal. The diffraction efficiency of ionomers with Cu^{2+} is much smaller, particularly with 6 mol % of Cu^{2+} for whose grating is merely discernible. We performed a number of experiments using different conditions including smaller period of grating of 2 μm; although absolute values may vary, the observations as discussed from Figures 9 and 10 were very much reproducible. For instance, the film of Azo-0.14MA-0.06Zn used for the experiment in Figure 10 was thicker (2.5 μm) than that of the film used for Figure 9 (1.8 μm), while the calculated refractive index modulation of the grating after 5 min excitation was about the same ($\Delta n = 0.021$).

The fact that only the ionomers with a significant increase in T_{ni} showed higher photoinduced birefringence and stronger diffraction efficiency of holographic grating seem to indicate that the thermal stability of the nematic phase in the presence of metal ions determines the degree of photoalignment of azobenzene mesogens. This may imply less important thermal relaxation of azobenzene mesogens occurred during the

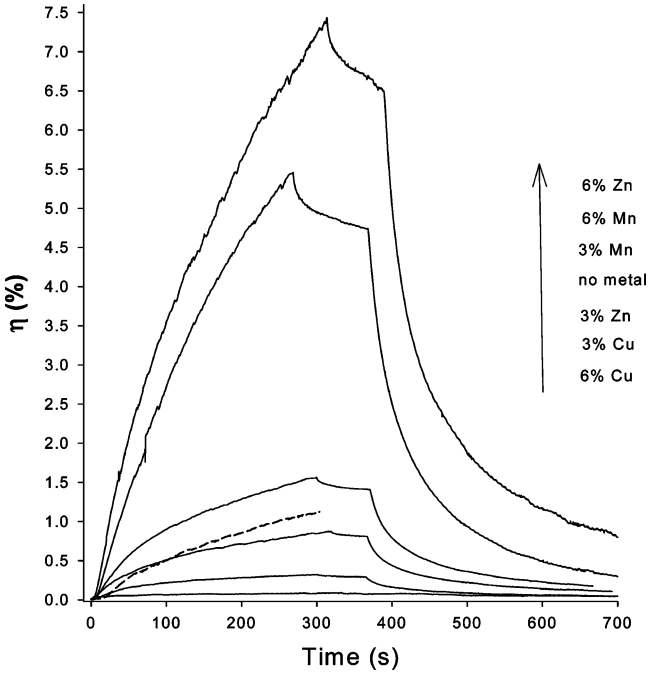

Figure 10. First-order (+1) diffraction efficiency vs time for gratings (5 μm period) recorded in films of Azo-0.26MA and its ionomers with 3 and 6 mol % of Zn^{2+}, Mn^{2+}, and Cu^{2+} ions, the excitation intensity (Ar^+ laser, 488 nm) being 50 mW/cm^2 per recording beam.

photoalignment process when the nematic phase is thermally more stable, since photoinduced anisotropy in azobenzene polymers generally becomes smaller with increasing the temperature of measurement as a result of thermal relaxation.[13] However, we stress that the underlying mechanism responsible for the effect of metal ions on the photoinduced anisotropy may be much more complicated than the apparent correlation with the effect of metals on the thermal stability of the LC phase and needs further investigations to understand. The morphology of ionomers, which is a complex issue on its own,[10,20]may well play a role in the photoalignment process of azobenzene ionomers.

Conclusions

Two series of azobenzene-containing liquid crystalline ionomers were prepared and characterized. It was found that using methacrylic acid for neutralization with metal ions, ionomers with Zn^{2+} and Mn^{2+}have increased thermal stability of the nematic phase formed by azobenzene mesogens, even though the LC order as revealed by the nematic-to-isotropic phase transition enthalpy is reduced by the presence of metal ions. When this happens, ionomers display an increased photoinduced birefringence, and consequently, their holographic gratings produced by an interference pattern with polarization modulation exhibit significantly enhanced diffraction efficiency. Such improvement of these optical properties could not be obtained for ionomers for which the presence of metal ions or ionic aggregates destabilizes or has little effect on the thermal stability of the LC phase. The finding reported in this paper suggests that exploring the insertion of metal ions in azobenzene liquid crystalline polymers may be an effective way to improve or to tune the properties of azobenzene polymers.

Acknowledgment. The authors thank Dr. Li Cui, Ms. Milène Lécorché, and Mr. Christophe Pinot for their help in some early experiments and Prof. Pierre Harvey (Sherbrooke) for helpful discussions. Financial support from the Natural Sciences and Engineering Research Council of Canada and le Fonds québécois de la recherche sur la nature et les technologies of Québec is also acknowledged.

References and Notes

(1) Lei, H.; Zhao, Y. *Polym. Bull. (Berlin)* **1993**, *31*, 645.
(2) Zhao, Y.; Lei, H. *Macromolecules* **1994**, *27*, 4525.
(3) Roche, P.; Zhao, Y. *Macromolecules* **1995**, *28*, 2819.
(4) Wiesemann, A.; Zentel, R.; Pakula, T. *Polymer* **1992**, *33*, 5315.
(5) Pabmann, M.; Wilbert, G.; Cochin, D.; Zentel, R. *Macromol. Chem. Phys.* **1998**, *199*, 179.
(6) Barmatov, E.; Prosvirin, A.; Barmatova, M.; Galyametdinov, Y.; Haase, W.; Shibaev, V. *Macromol. Rapid Commun.* **2000**, *21*, 281.
(7) Barmatov, E.; Pebalk, D.; Barmatova, M.; Shibaev, V. *Macromol. Rapid Commun.* **2000**, *21*, 369.
(8) Barmatov, E.; Pebalk, D.; Barmatova, M.; Shibaev, V. *Polymer.* **2002**, *43*, 2875.
(9) Barmatov, E.; Barmatova, M.; Bong-Seok, M.; Jae-Geun, P. *Macromolecules* **2004**, *37*, 5490.
(10) Grady, B. P.; Goossens, J. G. P.; Wouters, M. E. *Macromolecules* **2004**, *37*, 8585.
(11) Ichimura, K. *Chem. Rev.* **2000**, *100*, 1847.
(12) Viswanathan, N.; Kim, D. Y.; Bian, S.; Williams, J.; Liu, W.; Li, L.; Samuelson, L.; Kumar, J.; Tripathy, S. K. *J. Mater. Chem.* **1999**, *9*, 1941.
(13) Natansohn, A.; Rochon, P. *Chem. Rev.* **2002**, *102*, 4139.
(14) Ikeda, T. *J. Mater. Chem.* **2003**, *13*, 2037.
(15) (a) Bai, S.; Zhao, Y. *Macromolecules* **2002**, *35*, 9657. (b) Leclair, S.; Mathew, L.; Giguere, M.; Motallebi, S.; Zhao, Y. *Macromolecules* **2003**, *36*, 9024. (c) Cui, L.; Tong, X.; Yan, X.; Liu, G.; Zhao, Y. *Macromolecules* **2004**, *37*, 7097. (d) Wang, G.; Tong, X.; Zhao, Y. *Macromolecules* **2004**, *37*, 8911.
(16) Portugal, M.; Ringsdorf, H.; Zentel, R. *Makromol. Chem.* **1982**, *183*, 2311.
(17) Cloutier, S.; Peyrot, D.; Galstian, T.; Lessard, R. *J. Opt. A: Pure Appl. Opt.* **2002**, *4*, S228.
(18) Zhao, Y.; Bai, B.; Asatryan, K.; Galstian, T. *Adv. Funct. Mater.* **2003**, *13*, 781.
(19) *Liquid Crystalline Polymers*; Donald, A. M., Windle, A. H., Eds.; Cambridge University Press: New York, 1992.
(20) Eisenberg, A.; Hird, B.; Moore, R. B. *Macromolecules* **1990**, *23*, 4098.
(21) Cui, L.; Zhao, Y.; Yavrian, A.; Galstian, T. *Macromolecules* **2003**, *36*, 8246.
(22) Yoneyama, S.; Yamamoto, T.; Tsutsumi, O.; Kanazawa, A.; Shiono, T.; Ikeda, T. *Macromolecules* **2002**, *35*, 8751.

MA0473869